VOLUME 59 NUMBERS 3–4 2003

ISSN 0040-2508

TELECOMMUNICATIONS AND RADIO ENGINEERING

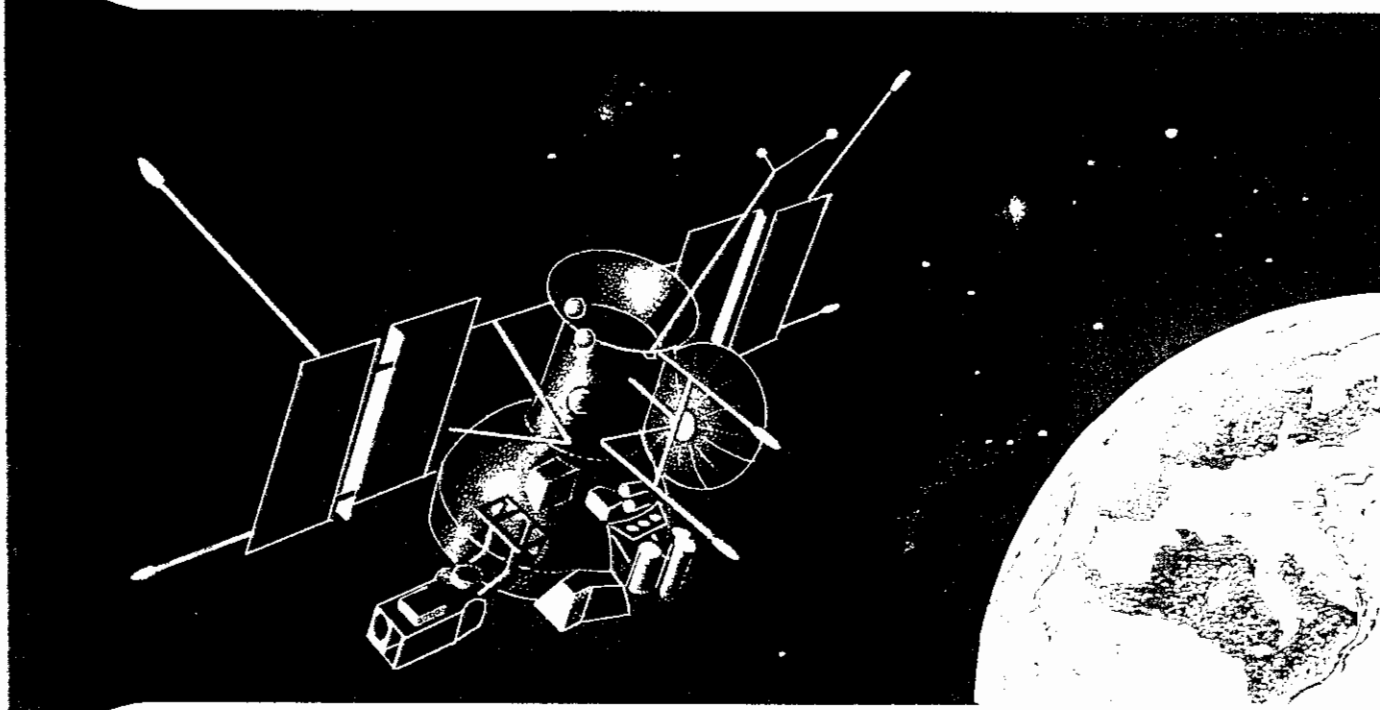

Published by Begell House, Inc.

Evaluation of Size of the Atmospheric Aerosol Particles in the Reflecting Layers Occurring after Intense Solar Flares*

Yu.V. Goncharenko and F.V. Kivva

A. Usikov Institute of Radio Physics and Electronics, National Academy of Sciences of Ukraine
12, Academician Proskura St., Kharkov 61085, Ukraine

The hypothesis for the effect of aerosol layers emerging after intense solar flares on variations in the temperature profile of lower and middle atmosphere is considered. Estimated aerosol particle size does not contradict the water aerosol physics and approximately corresponds to the maximum of the Dermidzhyan H-distribution for altitude and stratospheric aerosols.

The effect of solar activity on weather and climate has been attracting considerable researcher's attention for more than a century. However, the models adequately explaining this effect have not yet been suggested. The variations in the total flux of solar radiation, referred to as the solar constant, are known to be 0.1-0.2%. This constant is much less than 1-2%, the value needed for the direct influence of solar activity on weather [1, 2]. Nevertheless, a plenty of evidence indicates that variations in solar activity account for the Earth's weather and climate changes [1, 2]. An assumption can be made that there exist some nonlinear mechanisms, particularly, those associated with the moisture phase transitions, by which weak external impacts can promote fast release of the energy stored by the atmosphere. In elucidating these mechanisms it is important to ascertain how the variations of the solar (SCR) and galactic cosmic rays (GCR) can affect the troposphere parameters.

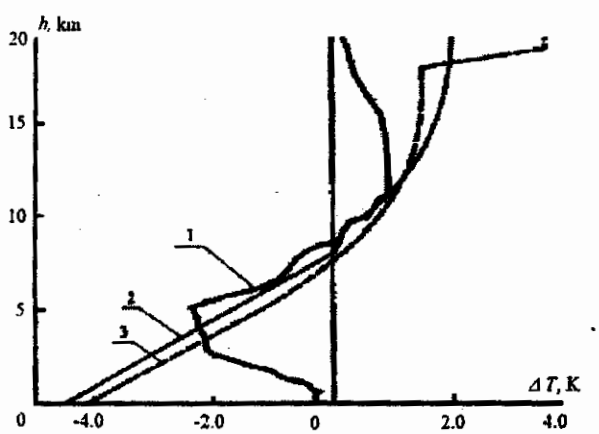

Fig. 1. Changes in the temperature profile of the lower and middle troposphere:
1 - experiment; 2 – model with the 8-9 km – level reflecting layer;
3 – model with the 14-16 km – level absorbing layer

* Originally published in *Radiophysics and Electronics*, Vol. 7, No 3, 2002, pp. 509–512.

ISSN0040-2508

Experimental studies have revealed that the altitude temperature profile of the middle and lower atmosphere undergoes changes following intense solar flares. Fig. 1 (curve 1) refers to the changes of the atmospheric temperature (ΔT) after a solar flare [3]. Theoretical calculations performed within the framework of one-dimensional planar atmosphere model [3] allowed this phenomenon to be explained in terms of the reflecting and absorbing layers being formed at altitudes from 5 to 20 km. A good agreement between the numerical simulation and experimental data in the 5-15 km altitude range was obtained for the 8-9 km – level reflecting layer (Fig. 1, curve 2) or 14-16 km – level absorbing layer (Fig. 1, curve 3) whose transmission coefficients were around 90%.

It is evident that absorption of the solar energy by a certain layer resulted in the atmosphere warming-up at the altitude of this layer (the 10-20 km altitude range in Fig. 1) and its cooling at lower altitudes.

Similarly, Fig. 1 illustrates that the atmosphere is cooled under the reflecting layer formed at the altitudes 8-9 km and warmed-up above it.

Consider the reflecting-layer model. This layer may consists of macromolecular complexes comprising the ions of atmospheric gas and water molecules. It is known that high-energy SCR and GCR modulated by the solar wind variations may be a source of ions and radicals at altitudes of 8-20 km [2]. The mechanism underlying the formation of these ions and coupled aerosol particles is depicted in Fig. 2 [4]. The high-energy SCR flux density increased within 1-2 hours since the solar flare beginning, whereas a decrease in the SCR intensity, referred to as Forbush-effect, occurs after 24-48 h or more since its commencement.

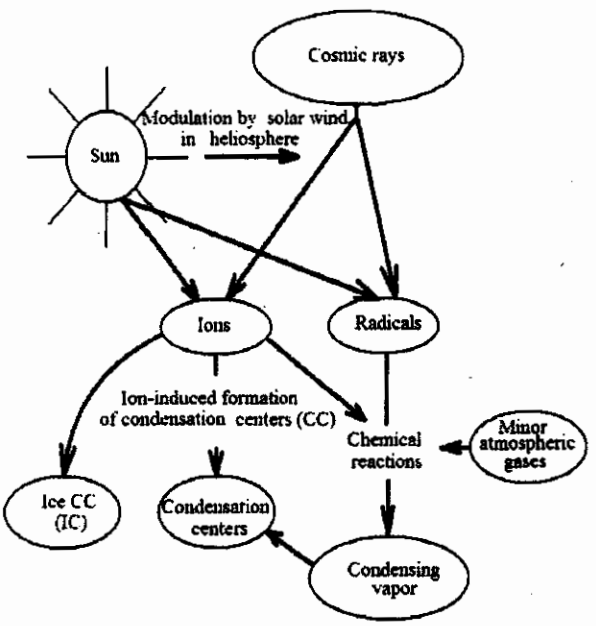

Fig. 2. Relation of GCR and SCR to the formation of atmosphere aerosol particles

These aerosol particles can turn into the atmospheric vapor condensation centers at low or negligible degrees of over-saturation [5]. This fact can be attributed to the lower pressure of water vapor above the charged drop surface, compared to that for the uncharged drop [6] .

Let us assume that the aerosol concentration N is proportional to the ion concentration at this altitude. Since it can vary between 100 and 1000 cm^{-3} during the intense solar flare [2], the aerosol concentration will likewise increase by approximately an order of magnitude.

It is known that 98% of solar energy falls in the 0.2 - 3 μm waveband [7] (Fig. 3), and this energy is close to being time-invariant. Thus, one should consider the effect of atmospheric aerosol on the electromagnetic energy transfer occuring mainly within the above waveband.

An important parameter specifying the substance behavior in an electromagnetic field is its dielectric permittivity ε.

$$\varepsilon = \varepsilon' - i\varepsilon'', \tag{1}$$

where ε' accounts for the polarization properties of a substance; and ε'' characterizes absorption of electromagnetic energy by a substance

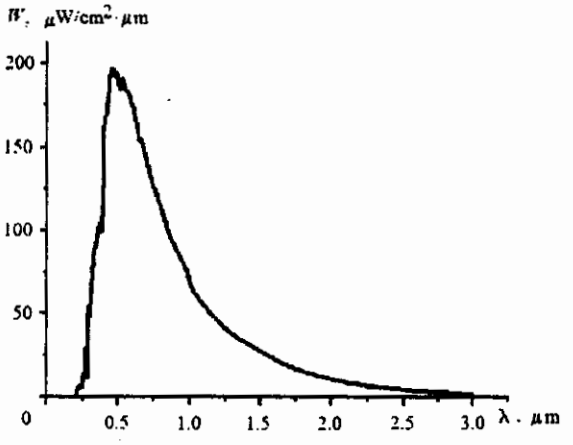

Fig. 3. $W(\lambda)$ – spectrum of solar energy flux

Within the waveband under study the dielectric permittivity of pure water is ε = 1.322-i0.00001 [8]. Because of the small value of imaginary part we will restrict ourselves to analyzing the mechanism of the drop scattering without evaluating the electromagnetic energy absorption by the drops.

Evaluation of the size of atmospheric aerosol particles in a reflecting layer

The size of atmospheric aerosol particles is known to vary strongly depending on their nature and formation conditions. Since this size may be comparable with a wavelength, the electromagnetic wave scattering on the aerosol particles must be calculated according to the Mi equation

$$K_{bs}(\varepsilon, x) = \frac{2}{\pi^2}\sum_{n=1}^{\infty}(2n+1)(|a_n|^2 + |b_n|^2), \tag{2}$$

where

$$x = \frac{2\pi r}{\lambda}; \tag{3}$$

$$a_n = \frac{A_n(\varepsilon x)\psi_n(x) - \varepsilon\psi_n'(x)}{A_n(\varepsilon x)\xi_n(x) - \varepsilon\xi_n'(x)},$$
$$b_n = \frac{\varepsilon A_n(\varepsilon x)\psi_n(x) - \psi_n'(x)}{\varepsilon A_n(\varepsilon x)\xi_n(x) - \xi_n'(x)}; \quad (4)$$

$$\psi_n(x) = \sqrt{\frac{\pi x}{2}} J_{n+1/2}(x); \quad (5)$$

$$\xi_n(x) = \sqrt{\frac{\pi x}{2}} [J_{n+1/2}(x) + (-1)^n i J_{-n-1/2}(x)]; \quad (6)$$

$$A_n(\varepsilon x) = \frac{\psi_n'(\varepsilon x)}{\psi(\varepsilon x)}. \quad (7)$$

Here $J_{n\ 1/2}$ and $J_{-n-1/2}$ are the Bessel functions; $\varepsilon = \varepsilon' - i\varepsilon'' = = 1.322 - i0.00001$ – complex dielectric permittivity of water in the 0.2 - 3 μm waveband; $\xi' = \frac{d\xi}{dx}$, $\psi' = \frac{d\psi}{dx}$ are x partial derivatives.

To calculate the Mi coefficients a_n and b_n (4,7) the Dermidzhyan algorithm optimized to reduce the computer calculation time has been used [8].

The propagation factor (dB/km) has been determined according to the Bouger law

$$\alpha_{scat}(x,\varepsilon) = 1.346439 \cdot 10^{-2} \times \int_{R_1}^{R_2} r^2 N f(r) K_{bs}(x,\varepsilon) dr, \quad (8)$$

where N is the aerosol concentration (cm^{-3}); r is the drop radius (μm); $f(r)$ is the drop size distribution.

To make rough calculations let us assume that the diameter of atmospheric aerosol drops is constant because of the similar physical conditions of their formation.

Over the 0.2 - 3 μm waveband the integral factor of electromagnetic wave attenuation by a layer $V(r)$ is defined as (9)

$$V(r) = \frac{1}{W_0} \int_{\lambda_1}^{\lambda_2} K_{scat}(\frac{2\pi r}{\lambda}, \varepsilon) W(\lambda) d\lambda, \quad (9)$$

where W_0 is the solar constant ($W_0 = 1373 \pm 20$ W/m^2 [7]); $W(\lambda)$ is the solar energy spectrum.

Experimental studies of these layers performed at the Max Planck Institute for Meteorology (Hamburg) have revealed that the layer thickness may vary in the range 0.5 – 1.5 km [9]. An example of this layer is given in Fig. 4.

The data have been obtained with the 1064 nm – lidars in Barcelona and Hamburg on September 12, 2000 during the solar flare [9]. As seen in Fig. 4, the layer of strong scattering is located at altitudes of 10-12 km. Unfortunately, the reported experimental data permit evaluation of the aerosol layer thickness only (around 1.5 km) with its power remaining unknown.

Presented in Fig. 5 are the results of the transparency coefficient (W) calculations for the 1 km – thickness reflecting layer with aerosol particle concentration being 100 cm^{-3} before the flare (curve 1), and 1000 cm^{-3} after the flare (curve 2). As seen in Fig. 5, the layer does not exert a significant influence

Conclusions

As shown in Fig. 5, the tentative average size of aerosol particles 0.2 μm, (point 1 in Fig. 6) is not in conflict with the physical nature of water aerosols and approximately corresponds to the maximum of Dermidzhyan haze «H» distribution [10] shown in Fig. 6 for the altitude and stratospheric aerosols.

Thus, the ions produced in the upper troposphere by the high-energy SCR and the water vapor condensed on these ions can bring about experimentally detectable changes in the altitude temperature profile of the lower atmosphere. These phenomena are responsible for the local changes of the isobaric surface altitudes, thereby giving rise to the additional vertical and horizontal pressure gradients. They may cause the formation of the near-ground and elevated tropospheric ducts which play an essential role in radiowave propagation.

The results from the studies discussed above are of certain importance since they corroborate the mechanism behind the SCR effect upon the tropospheric meteoparameters. It is exactly owing to this mechanism that an insignificant SCR external action not exceeding 0.1% of the solar constant may lead to a 10% decrease of the total energy entering the troposphere.

References

1. Мирошниченко Л.И. Солнечная активность и Земля (Solar activity and Earth) - М.: Наука, 1981. – 95 с.
2. Солнечно-земные связи, погода и климат (Sun-Earth relations, weather and climate) / Под ред. Б.Мак-Кормака и Т.Семеги. - М.: Мир, 1982. – 376 с.
3. Пудовкин М.И., Дементьева А.Л. Вариации высотного профиля температуры в нижней атмосфере во время солнечных событий (Variations of the altitude temperature profile in lower atmosphere during the sun events) // Геомагнетизм и аэрономия. - 1997. – Т. 37, №3. – С.84-91.
4. European organization for nuclear research. A study of the link between cosmic rays and clouds with cloud chamber at the Cern Ps. // SPSC, 24 April 2000. – 107 p.
5. Raes F., Janssens A., Dingenen R.V. The role of ion-induced aerosol formation in the lower atmosphere // J. Aerosol Sci. – 1986. – No 17. – P.466-472.
6. Дас Гупа Н.Н., Гош С.К. Камера Вильсона и ее применение в физике. (Wilson chamber and its application in physics.) - М.: Изд-во иностр. лит., 1947. – 162 с.
7. Оран. Р. Вайт. Поток солнечного излучения и его вариации. (Solar radiation flux and its variations.) - М.: Мир, 1980. – 418 с.
8. Дейрменджан Д. Рассеяние электромагнитного излучения сферическими полидисперсными частицами. (Scattering of electromagnetic radiation at spherical polydisperse particles.) - М.: Мир, 1971. – 165 с.
9. Max Planck Institute for Meteorology. Report N337 «Lidar intercomparisons on algorithm and system level in frame of EARLNET» by Volker Mattias et al. Hambugr, May 2002. – 67 p.
10. Айвазян Г.М. Распространение миллиметровых и суб-миллиметровых волн в облаках. (Propagation of millimeter and sub-millimeter waves in clouds.) - Л: Гидрометеоиздат, 1991. – 479 с.